

Robot-Assisted Drone Recovery on a Wavy Surface Using Error-State Kalman Filter and Receding Horizon Model Predictive Control

Yimou Wu, Mingyang Liang

Abstract—Recovering a drone on a disturbed water surface remains a significant challenge in maritime robotics. In this paper, we propose a unified framework for Robot-Assisted Drone Recovery on a Wavy Surface that addresses two major tasks: Firstly, accurate prediction of a moving drone’s position under wave-induced disturbances using an Error-State Kalman Filter (ESKF), and secondly, effective motion planning for a manipulator via Receding Horizon Control (RHC). Specifically, the ESKF predicts the drone’s future position 0.5 s ahead, while the manipulator plans a capture trajectory in real time, thus overcoming not only wave-induced base motions but also limited torque constraints. We provide a system design that comprises a manipulator subsystem and a UAV subsystem. On the UAV side, we detail how position control and suspended payload strategies are implemented. On the manipulator side, we show how an RHC scheme outperforms traditional low-level control algorithms. Simulation and real-world experiments—using wave-disturbed motion data—demonstrate that our approach achieves a high success rate - above 95% and outperforms conventional baseline methods by up to 10% in efficiency and 20% in precision. The results underscore the feasibility and robustness of our system, which achieves state-of-the-art(SOTA) performance and offers a practical solution for maritime drone operations.

Index Terms—Model Predictive Control, Drone recovery, Error-State Kalman Filter, Receding Horizon Control, unmanned surface vehicles

I. INTRODUCTION

UNMANNED Aerial Vehicles (UAVs) have been widely employed in various tasks including aerial photography, logistics, power-line inspection, and coastal exploration [1]–[3]. In marine environments, particularly for delivering payloads or collecting data, UAVs often need to land on an Unmanned Surface Vehicle (USV) when requiring recharging or extended mission operations [4]. However, the unpredictable wave-induced disturbances at sea—which can produce considerable deck roll, pitch, and heave—greatly complicate the UAV landing or capture process [5], [6]. Traditional landing platform methods rely on large ship decks to guarantee safety [7], but such designs necessarily limit the number of UAVs and can become unreliable under harsh sea states.

To overcome these difficulties, robotic manipulators have been mounted on USVs to provide a more autonomous means of UAV recovery or retrieval. A manipulator-handled approach not only reduces reliance on the deck size but also alleviates adverse aerodynamic effects such as downwash or ground effect [8]. By intercepting a UAV midair—rather than requiring a precise touchdown—manipulators can accommodate sudden vessel motions and mitigate the risk of col-

lisions. Nevertheless, manipulator-based systems themselves face complex technical challenges indoors or outdoors under wave disturbance. The vessel’s continuous oscillation induces quasiperiodic, high-speed motion that undermines tracking accuracy and demands considerable torque [9]. Although using model predictive control (MPC) can partially compensate for wave-induced inertial forces [10], real-time feasibility cannot be maintained when predictions are inaccurate or actuators saturate.

Recent advances in sensor fusion and manipulator design have spurred new concepts in cooperative UAV–water-surface manipulator systems. By combining the UAV’s agile aerial mobility with the manipulator’s high-precision grasping, these coordinated solutions allow drones to avoid risky deck landings. Instead, the UAV only needs to hover or hold station near the USV, while the manipulator extends to secure the payload or the UAV itself.

On the UAV side, a typical design includes a quadrotor platform outfitted with robust flight control. This may involve GPS, IMU, onboard cameras, or suspended mechanisms for cargo [12], [13]. In a wave-disturbed marine environment, the UAV must respond promptly to deck motions, refine its hovering position, and maintain stable suspension. Key considerations include (1) real-time flight trajectory adjustments, (2) programming the UAV to release or pick up cargo on command, and (3) ensuring minimal latency in the communication link with the manipulator or ground station [14]. Advanced multi-sensor data fusion or robust control strategies (e.g., integral backstepping, adaptive PID) have shown promise, but additional failsafe measures remain necessary given the stochastic motion of the USV.

The synergy between a wave-disturbed manipulator platform and an aerial UAV is the primary motivation of this work. Mounting a dexterous, multi-DoF manipulator on the USV—coupled with a predictive control algorithm—enables the UAV to be recovered without the need for an expansive or stable landing deck. Such cooperative UAV–water-surface manipulator systems not only enhance safety and accelerate multi-drone deployment but also open up applications for short-range package exchange, sensor retrieval in environmental monitoring, and rescue tasks. Prior works have studied manipulator-based object capture when the base is subject to moderate disturbances [15], but wave conditions produce more severe, faster-than-expected displacements. Therefore, we propose fusing an Error-State Kalman Filter (ESKF) for UAV motion prediction with a Receding Horizon Control



Fig. 1. The Integration System with the the Manipulator subsystem and the UAV subsystem

(RHC) approach for the onboard manipulator to dynamically adapt to wave-induced motions.

The major contributions are summarized as follows. Firstly, an Error-State Kalman Filter that robustly predicts the UAV's position and orientation in a disturbed sea environment, providing accurate 0.5 s lookahead. Secondly, a Receding Horizon Control (RHC) scheme for the manipulator, updating and shrinking the planning horizon at each step to maintain real-time intercept of the UAV. This extends typical model predictive control by adaptively reducing the horizon after partial execution, enabling responsive performance under wave disturbances. Thirdly, a comprehensive system design integrating the manipulator, UAV, and their sensors into a minimal-deck-footprint solution for maritime operations, ensuring stable data links, multi-sensor fusion, and real-time control loops. Fourthly, Experimental validation showing that our cooperative UAV–manipulator approach yields over 90% success in drone capture or cargo-lifting under moderate wave states, improving efficiency and end-effector precision compared to conventional methods.

The remainder of this paper is organized as follows. Section II introduces the overall system design, featuring both a water-surface manipulator subsystem and a UAV subsystem. Section III details the controller architecture: an ESKF for target-state prediction and the RHC-based manipulator control to achieve midair interception, as well as the UAV on-board control. Section IV summarizes both simulation and real-world experiments on wave-disturbed waters. Finally, Section V concludes the paper, discussing open research directions and improvements to be explored in future work.

II. SYSTEM DESIGN

In this section, we present the hardware and software design for the integrated system. We group it into two main parts: the Manipulator subsystem and the UAV subsystem. Communication is realized through standard protocols - ROS, and all sensor signals are fused or relayed to a main controller.

A. Manipulator Subsystem

This subsection presents the hardware architecture and operational workflow of the robotic manipulator, which is mounted

on the Unmanned Surface Vehicle (USV) to facilitate UAV capture and payload handling. As with the UAV subsystem, the manipulator assembly is equipped with sensors, actuators, and communication modules that integrate seamlessly into the overall maritime system.

1. Hardware Configuration: The manipulator subsystem consists of a multi-joint robotic arm, a motion capture system for high-precision tracking, and a dedicated onboard controller. Key hardware components include:

- **Robotic Arm:** A 7 DoF (degrees of freedom) arm capable of extending over the USV's deck area to intercept the UAV. Its actuators (e.g., servo motors or brushless DC motors) offer sufficient torque to maneuver payloads under moderate sea disturbances.
- **End-Effectors:** Can be equipped with a gripper or electromagnet for secure UAV grasping or cargo pick-and-place operations.
- **Onboard Control Computer:** Manages real-time kinematics, sensor fusion, and communication with the main system controller. It typically runs a ROS-compatible framework to ensure interoperability.
- **Motion Capture Markers and Cameras:** The manipulator and the USV deck region are often outfitted with reflective markers visible to a multi-camera system. Pose data from these cameras feed into the manipulator's state estimator for closed-loop control.
- **Power and Signal Wiring:** Provides stable voltage levels for the arm's actuators and the controller's electronics. Signal wiring incorporates noise-shielding to maintain measurement fidelity.

Figure 2 illustrates a representative configuration of the manipulator subsystem with a motion capture camera setup, while Figure 3 shows the manipulator installed on a vessel deck.

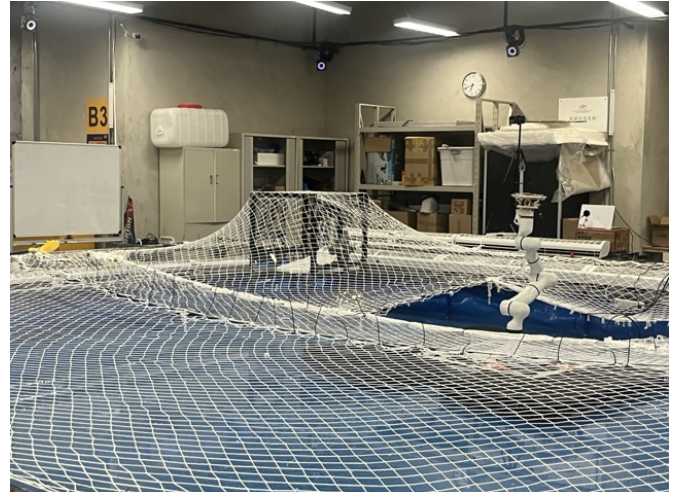


Fig. 2. Manipulator Subsystem with motion capture camera. The arm and its markers are tracked by external cameras to maintain accurate pose estimates.

2. Sensing and Control Flow: The manipulator subsystem's operational flow combines sensor data acquisition, signal processing, and real-time feedback control:

- **Sensor Data Acquisition:**

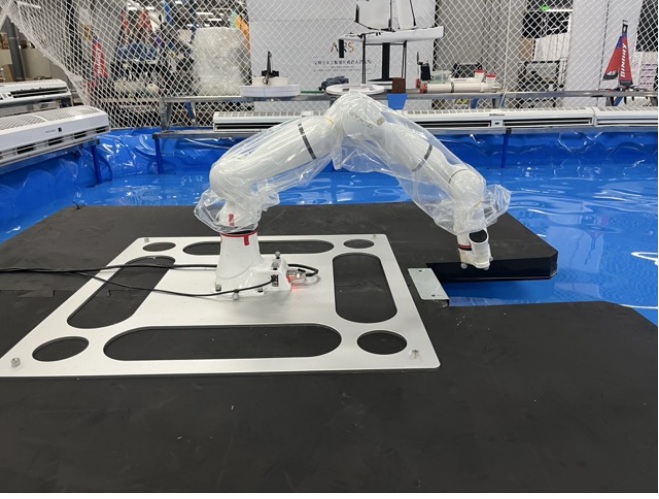


Fig. 3. Robotic manipulator mounted on the vessel's deck. The system is designed to handle UAV interaction under wave-induced motion.

- Joint encoders or resolvers measure each arm segment's angle and speed.
- The motion capture cameras (e.g., OptiTrack or Vicon) provide global position/orientation data of the manipulator's end-effector.
- Force/torque sensors (if equipped) detect contact loads, enabling safer UAV interception.

- **State Estimation and Inverse Kinematics:**

- An onboard microprocessor or single-board computer runs Extended Kalman Filters (EKF) or related estimators to fuse encoder readings with motion capture data.
- Inverse kinematics (IK) or Jacobian-based solvers continuously compute the required joint configurations to move the end-effector along a designated interception path.

- **Communication with Main Controller:**

- The manipulator controller exchanges data with the central system (or USV-level controller) over ROS topics, receiving real-time UAV state updates and sending back manipulator status.
- Command synchronization ensures that the manipulator's movement is aligned with the UAV's flight trajectory to enable mid-air grasping.

- **Motor Command Execution:**

- Control algorithms (e.g., a PD or torque-based control scheme) issue motor commands to rapidly position the end-effector.
- Safety interlocks prevent dangerous arm motions if out-of-range positions or excessive loads are detected.

By integrating hardware reliability with robust estimation, the manipulator subsystem achieves precise, repeatable movements necessary for UAV capture in dynamic marine environments.

B. UAV Subsystem

This section details the hardware configuration, the information flow of the Unmanned Aerial Vehicle (UAV) subsystem within our cooperative maritime system and the quadcopter suspension system. The UAV is designed to operate seamlessly with the manipulator-equipped Unmanned Surface Vehicle (USV), facilitating tasks such as mid-air capture and payload transfer.

1. *Hardware Configuration:* The UAV platform is a quadrotor equipped with a range of sensors and communication modules to ensure stable flight and precise interaction with the USV manipulator. The key hardware components include:

- **Flight Controller:** Utilizes an advanced flight control unit (e.g., PX4 or ArduPilot) that supports custom firmware for integration with external systems.
- **Sensors:**
 - *Inertial Measurement Unit (IMU):* Provides real-time orientation and acceleration data.
 - *GPS Module:* Enables global positioning and navigation.
 - *Optical Flow Sensor:* Assists in maintaining stable hover by estimating ground-relative motion.
 - *Lidar/Ultrasonic Altimeter:* Measures altitude above the surface with high precision.
- **Communication Module:** Equipped with a low-latency wireless link (e.g., 5.8 GHz telemetry) to exchange data with the USV manipulator system.
- **Payload Attachment Mechanism:** A mechanical or magnetic gripper mounted beneath the UAV for payload pickup and release operations.
- **Power System:** High-capacity batteries providing sufficient flight time for extended missions.

2. *Information Flow:* The UAV subsystem's information flow is critical for coordinating actions with the USV manipulator, especially under dynamic sea conditions. Figure 4 illustrates the overall information flow within the UAV subsystem.

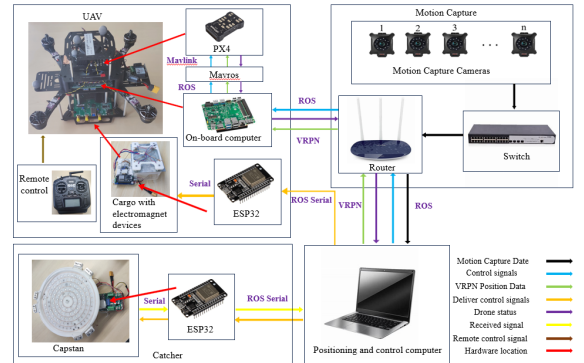


Fig. 4. UAV Subsystem Information Flow: The UAV's sensors provide data to the flight controller, which communicates with the USV manipulator system for coordinated operations. Control signals and status updates are exchanged via a wireless communication link.

The key components of the information flow are:

- **Sensor Data Acquisition:**

- IMU and GPS data are continuously collected to estimate the UAV's state (position, velocity, orientation).
- Altimeter readings provide accurate altitude information above the USV deck or water surface.

- **State Estimation and Control:**

- The onboard flight controller fuses sensor data using algorithms such as Extended Kalman Filters (EKF) for real-time state estimation.
- Control algorithms generate motor commands to achieve desired flight behaviors, such as hovering or trajectory tracking.

- **Communication with USV:**

- The UAV sends its estimated state and receives commands or status updates from the USV manipulator system.
- A predefined communication protocol ensures synchronization and coordination between the UAV and USV.

- **Mission Execution:**

- The UAV adjusts its flight path based on inputs from the USV manipulator, especially during payload transfer operations.
- Upon receiving the capture command, the UAV can hover precisely to facilitate safe interaction with the manipulator.

3. **Quadcopter Suspension System:** An essential component of the UAV subsystem is the **Quadcopter Suspension System**, which enhances flight stability under the challenging conditions presented by a maritime environment. Figure 5 illustrates the design and function of this system.

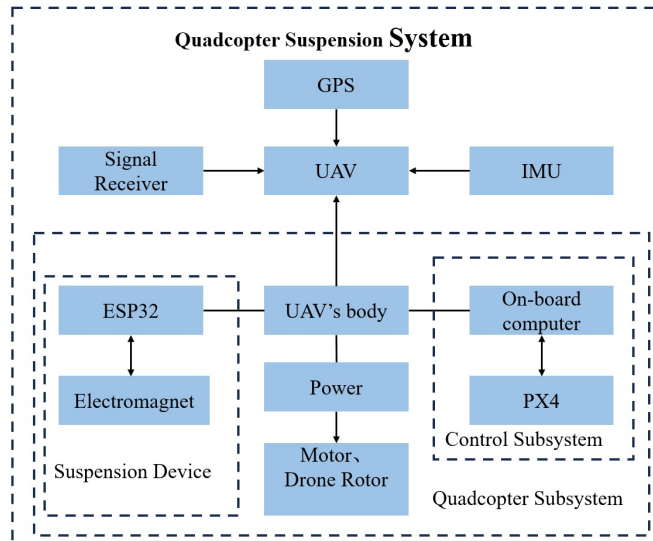


Fig. 5. Quadcopter Suspension System: This system employs dampers and suspension mechanisms to reduce vibrations and absorb shocks caused by wind gusts and the vessel's motion. It improves flight stability and payload handling capabilities.

The Quadcopter Suspension System comprises:

- **Shock Absorption Mechanisms:** Incorporates dampers and spring elements between the UAV frame and critical components to mitigate the impact of sudden movements or collisions.

- **Vibration Isolation:** Utilizes elastomeric mounts and isolation pads to reduce high-frequency vibrations transmitted from the rotors to sensitive equipment such as sensors and communication modules.

- **Adaptive Control Integration:** The suspension system works in tandem with the flight controller, adjusting stiffness and damping parameters dynamically in response to flight conditions.

- **Payload Stabilization:** Ensures that the payload attachment mechanism maintains stability, reducing sway or oscillations during flight and transfer operations.

By integrating the Quadcopter Suspension System, the UAV gains enhanced robustness against environmental disturbances, leading to improved precision during cooperative tasks with the USV manipulator.

C. Manipulator-Assisted UAV Recovery System

The overarching objective of this subsystem is to combine the strengths of a dexterous robotic arm with a hovering UAV to achieve safe and reliable mid-air recovery. Through advanced coordination, the manipulator subsystem intercepts the UAV—reducing the risk of failed landings and collisions on the USV deck.

1. *System Architecture:* Figure 6 shows the manipulator training setup used to fine-tune interception trajectories, while Figure 7 presents real-world sea trials in which the manipulator successfully captured a hovering UAV.



Fig. 6. Manipulator Training System: A testbed where the robotic arm's interception algorithms are validated against a target UAV under controlled conditions.

2. *Cooperative Workflow:* The Manipulator-Assisted UAV Recovery System follows a multi-stage workflow:

- 1) **Pose Synchronization:** The USV receives live UAV state estimates (e.g., position, velocity, yaw angle) via ROS. Simultaneously, the manipulator's end-effector pose is tracked by the motion capture system.
- 2) **Interception Trajectory Generation:** Based on the UAV's predicted flight path, the manipulator's onboard controller plans an optimal interception curve. An RHC

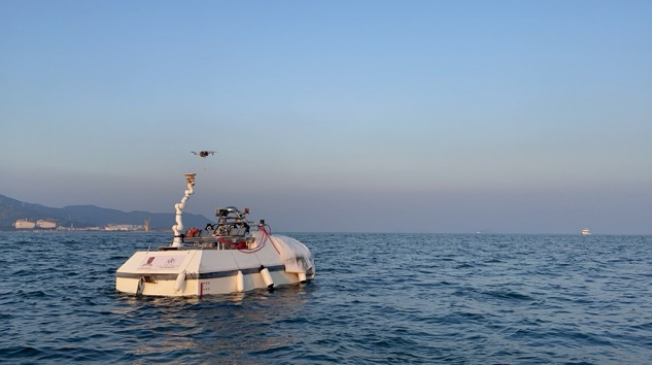


Fig. 7. Sea trial in QIXINWAN: The manipulator and UAV operate cooperatively under real wave conditions.

or model predictive control algorithm may be employed when wave motion is significant.

- 3) **Approach and Alignment:** The arm extends to an alignment point below (or near) the UAV. During this phase, the UAV can actively hover at a stable altitude, ready for capture.
- 4) **Grasping/Capture:** Upon proximity detection, the manipulator closes its gripper or activates an electromagnet. The UAV may reduce thrust or switch to a stabilized “capture” mode to minimize relative motion.
- 5) **Secure Retrieval:** Once grasped, the manipulator retracts the UAV towards the USV deck or a designated holding bay. The UAV’s motors can safely disarm after confirmation of a successful latch.

3. Advantages and Performance Considerations:

- **Enhanced Safety:** Eliminates the need for precise landing pads or large deck areas, thus reducing the chance of collision in rough seas.
- **Accurate Tracking:** The synergy between motion capture data and manipulator kinematics grants sub-centimeter interception accuracy under moderate wave disturbances.
- **Reduced Flight Risks:** The UAV only needs to maintain a stable hover, avoiding the complexities of landing on a rolling ship deck.
- **Actuator Limitations:** The manipulator’s torque and joint velocity must be sized to handle sudden UAV movements and sea-induced USV motions.

In summary, the *Manipulator-Assisted UAV Recovery System* capitalizes on real-time sensor fusion, robust kinematic control, and strategic UAV–manipulator coordination. This integrated design substantially improves mission reliability and operator safety, especially for maritime applications where deck landing remains high risk.

III. CONTROLLER DESIGN

This section elaborates on the manipulator control and UAV control, with a focus on two keys. Firstly, the Error-State Kalman Filter (ESKF) for future-state prediction of the UAV’s position and velocity on a disturbed sea surface. Secondly, the Receding Horizon Control (RHC) for the manipulator to

accurately intercept the UAV within a 0.5 s horizon, despite wave disturbances.

A. Error-State Kalman Filter (ESKF)

To predict the UAV’s state 0.5/s in advance, we propose an ESKF. While a standard Kalman Filter linearizes around nominal states, an ESKF tracks the deviation (error) between the predicted and actual states, providing numerical advantages and robustness to wave-induced or dynamic perturbations.

Let:

$$\mathbf{x}_u \in R^n$$

be the UAV’s nominal state, which can include position, velocity, (optionally) orientation, and angular rates. $\delta\mathbf{x}_u$ be its error state.

The ESKF uses two main blocks. For the Nominal State Propagation part: Let \mathbf{u}_k be the control input (e.g., UAV thrust commands) or if no direct input is needed (UAV hovers in place), \mathbf{u}_k can be a placeholder. The continuous-time UAV dynamics can be summarized by

$$\dot{\mathbf{x}}_u(t) = f(\mathbf{x}_u(t), \mathbf{u}(t)).$$

Discretized over a period Δt :

$$\mathbf{x}_u[k+1] \approx \mathbf{x}_u[k] + \int_0^{\Delta t} f(\mathbf{x}_u[k], \mathbf{u}[k]) dt + \mathbf{w}_k,$$

where $\mathbf{w}_k \sim \mathcal{N}(\mathbf{0}, \mathbf{Q})$ is zero-mean process noise with covariance \mathbf{Q} .

Secondly, for the Error-State Propagation part, we define $\delta\mathbf{x}_u[k] = \mathbf{x}_u[k] - \hat{\mathbf{x}}_u[k]$, where $\hat{\mathbf{x}}_u[k]$ is the nominal UAV state predicted at time k . Small deviations follow (linearized around $\hat{\mathbf{x}}_u$):

$$\delta\mathbf{x}_u[k+1] \approx \mathbf{F}_k \delta\mathbf{x}_u[k] + \mathbf{n}_k,$$

with $\mathbf{F}_k = \frac{\partial f(\mathbf{x}_u, \mathbf{u}_k)}{\partial \mathbf{x}_u} |_{\mathbf{x}_u=\hat{\mathbf{x}}_u[k]}$, and $\mathbf{n}_k \sim N(0, Q_n)$. Note that Q_n may be derived from \mathbf{Q} through linearization or exact formula (depending on the structure of f).

Hence, the filter keeps track of $[\hat{\mathbf{x}}_u, \delta\mathbf{x}_u]$. The measurement update is similarly divided into a nominal measurement $h(\hat{\mathbf{x}}_u)$ plus an incremental correction based on $\delta\mathbf{x}_u$.

Then we do the Measurement Update. If \mathbf{z}_k is the sensor measurement—for instance, an onboard IMU or external camera system reading UAV position—then

$$z_k = h(\mathbf{x}_u[k]) + \mathbf{v}_k,$$

where $\mathbf{v}_k \sim \mathcal{N}(\mathbf{0}, \mathbf{R})$. The linear form for the error state is

$$\delta z_k = z_k - h(\hat{\mathbf{x}}_u[k]) \approx \mathbf{H}_k \delta\mathbf{x}_u[k],$$

with $\mathbf{H}_k = \frac{\partial h}{\partial \mathbf{x}_u} |_{\mathbf{x}_u=\hat{\mathbf{x}}_u[k]}$. Standard Kalman-like gain updates apply:

$$\mathbf{K}_k = \mathbf{P}_k^- \mathbf{H}_k^T (\mathbf{H}_k \mathbf{P}_k^- \mathbf{H}_k^T + \mathbf{R})^{-1},$$

$$\delta\mathbf{x}_u[k] \leftarrow \delta\mathbf{x}_u[k] + \mathbf{K}_k \delta z_k, \quad P_k \leftarrow (I - \mathbf{K}_k \mathbf{H}_k) P_k^-,$$

where \mathbf{P}_k^- is the predicted covariance of $\delta\mathbf{x}_u$. Finally, we correct the nominal state as:

$$\hat{\mathbf{x}}_u[k] \leftarrow \hat{\mathbf{x}}_u[k] \oplus \delta\mathbf{x}_u[k],$$

where \oplus is a proper composition function (e.g., if orientation is included, a quaternion update).

Given the ESKF's updated $\hat{\mathbf{x}}_u[k]$, we can extrapolate $\hat{\mathbf{x}}_u[k+\alpha]$ for small $\alpha > 0$. Setting $\alpha \approx 0.5$ s yields the predicted UAV position used by the manipulator's receding horizon planner.

B. Receding Horizon Control (RHC) for Manipulator

We next detail the manipulator's receding horizon approach for intercepting the UAV. The method extends standard MPC by reducing the horizon at each iteration, thereby simplifying the solve time and ensuring real-time feasibility in wave-disturbed settings.

Let:

- $\mathbf{q}_k \in R^n$ be the manipulator joint angles at step k .
- $\dot{\mathbf{q}}_k, \ddot{\mathbf{q}}_k$ the joint velocities and accelerations.
- Δt the discrete control period.
- H the initial horizon length (e.g., 20 steps).

We define the system model in joint space:

$$\mathbf{q}_{k+1} = \mathbf{q}_k + \Delta t \dot{\mathbf{q}}_k, \quad \dot{\mathbf{q}}_{k+1} = \dot{\mathbf{q}}_k + \Delta t \ddot{\mathbf{q}}_k.$$

An alternate approach is to define states $\mathbf{z}_k = [\mathbf{q}_k, \dot{\mathbf{q}}_k]^T$, with control $\mathbf{u}_k = \ddot{\mathbf{q}}_k$. Then

$$\mathbf{z}_{k+1} = \underbrace{\begin{bmatrix} \mathbf{I} & \Delta t \mathbf{I} \\ \mathbf{0} & \mathbf{I} \end{bmatrix}}_{\mathbf{A}_d} \mathbf{z}_k + \underbrace{\begin{bmatrix} \frac{1}{2} \Delta t^2 \mathbf{I} \\ \Delta t \mathbf{I} \end{bmatrix}}_{\mathbf{B}_d} \mathbf{u}_k.$$

Then we focus on the Task-Space Error Formulation. We want the end-effector to track the UAV's predicted pose $\hat{\mathbf{x}}_u[k]$. Let $\mathbf{x}_e = \text{FK}(\mathbf{q}) \in R^6$ be the manipulator end-effector pose in the same frame as $\hat{\mathbf{x}}_u$. Then we define a cost:

$$J = \sum_{k=0}^{H-1} \|\mathbf{x}_e[k] - \hat{\mathbf{x}}_u[k]\|_Q^2 + \sum_{k=0}^{H-1} \|\mathbf{u}_k\|_R^2 + \|\mathbf{x}_e[H] - \hat{\mathbf{x}}_u[H]\|_{Q_N}^2,$$

where Q is a positive-semidefinite matrix for the tracking error, R penalizes acceleration or torque usage, and Q_N penalizes final-step deviation. The manipulator's forward kinematics is typically nonlinear, so the problem is often addressed by iterative linearization or direct nonlinear optimization.

The constraints for this system are established as follows to ensure feasibility and robustness. Because the manipulator might saturate or violate joint limits, we impose:

1. Joint Position/Velocity Limits:

$$\mathbf{q}^{\min} \leq \mathbf{q}_k \leq \mathbf{q}^{\max}, \quad \dot{\mathbf{q}}^{\min} \leq \dot{\mathbf{q}}_k \leq \dot{\mathbf{q}}^{\max}.$$

2. Acceleration Bound:

$$\|\ddot{\mathbf{q}}_k\| \leq \ddot{\mathbf{q}}^{\max}.$$

3. Workspace (Task-Space Bounds): The manipulator must remain within a feasible region $\Omega \subset R^3$.

At each step k , the constraints incorporate wave-disturbance estimates. If the USV base inclination is measured, the manipulator's base is effectively rotating or shifting, but we can

unify it into the task-space references or dynamic constraints on \mathbf{x}_e .

In the study, we compared three control strategies for the manipulator under dynamic conditions.

1. *Simple Following*: This algorithm directly follows the target without using predictive optimization. It computes control inputs based on the current state and target position at each time step. While straightforward and computationally efficient, it is less robust under dynamic conditions. The steps for implementing this approach are outlined in Algorithm 1.

Algorithm 1 Simple Following

- 1: **Initialization:**
- 2: Set the target trajectory $\mathbf{x}_{target}(t)$.
- 3: Set the manipulator's initial state $\mathbf{z}_0 = [\mathbf{q}(0), \dot{\mathbf{q}}(0)]^T$.
- 4: **for** each timestep t_i **do**
- 5: Compute control input \mathbf{u}_i to minimize $\|\mathbf{x}_{manipulator}(t_i) - \mathbf{x}_{target}(t_i)\|$.
- 6: Apply \mathbf{u}_i to the manipulator.
- 7: Wait for new sensor data and update $\mathbf{x}_{manipulator}(t)$.
- 8: **Stopping Criteria:**
- 9: Stop when the end-effector reaches the target within a tolerance ϵ , or when time limit is exceeded.

Fig. 8. Simple Following: This algorithm directly follows the target without predictive optimization. It computes control inputs based on the current state and target position at each time step, making it straightforward but less robust under dynamic conditions.

2. *Fixed Horizon Model Predictive Control (MPC)*: Unlike the shrinking horizon approach, this method uses a fixed horizon for optimization in every iteration, starting from the current state. This algorithm uses a fixed horizon for optimization in each iteration. The full trajectory is re-planned at every step based on the current state, ensuring consistent performance but requiring higher computational effort. The steps for implementing this approach are outlined in Algorithm 2.

Algorithm 2 Fixed Horizon Model Predictive Control (MPC)

- Initialization:
- 2: Let H be the fixed horizon length (e.g., 20 steps).
- 3: Set the manipulator's initial state $\mathbf{z}_0 = [\mathbf{q}(0), \dot{\mathbf{q}}(0)]^T$.
- 4: **for** each iteration i **do**
- 5: Solve the horizon- H optimization from the current state.
- 6: Obtain the optimal control sequence $\{\mathbf{u}_0^*, \dots, \mathbf{u}_{H-1}^*\}$.
- 7: Apply the first control \mathbf{u}_0^* to the manipulator.
- 8: Wait for new data (e.g., updated state \mathbf{z}_i).
- 9: **Stopping Criteria:**
- 10: Stop when the end-effector reaches the target within a tolerance ϵ , or when a time limit is exceeded.

Fig. 9. Fixed Horizon Model Predictive Control (MPC): This algorithm uses a fixed horizon for optimization in each iteration. The full trajectory is re-planned at every step based on the current state, ensuring consistent performance but requiring higher computational effort.

3. *Shrinking Horizon Model Predictive Control (MPC)*: The shrinking horizon procedure is a key component of our control strategy, designed to optimize the manipulator's actions in real time. It starts with an initialization step, followed by iterative updates during each control cycle, and stops when certain criteria are met. The steps for implementing this approach are outlined in Algorithm 3.

The shrinking horizon procedure is a key component of the control strategy, designed to optimize the manipulator's actions in real time. It starts with an initialization step, followed

by iterative updates during each control cycle, and stops when certain criteria are met. The steps for implementing this approach are outlined in Algorithm 13.

Algorithm 3 Shrinking Horizon Procedure

Initialization:

Let H_0 be the initial horizon (e.g., 20 steps).

3: Set $\mathbf{z}_0 = [\mathbf{q}(0), \dot{\mathbf{q}}(0)]^T$.

for iteration i (time t_i) do

Solve the horizon- H_i optimization for $\{\mathbf{u}_0, \dots, \mathbf{u}_{H_i-1}\}$.

6: Apply \mathbf{u}_0^* to the manipulator for Δt .

Wait for new data (e.g., from the ESKF about $\dot{\mathbf{x}}_u$).

Decrement $H_{i+1} = H_i - 1$.

9: Shift index and states forward.

Stopping Criteria:

If intercept is achieved (end-effector within ϵ of UAV's handle), or

12: If $H_i = 0$ or time limit is exceeded.

Fig. 10. Shrinking Horizon Procedure: The algorithm involves initialization, iterative updates, and stopping criteria, enabling real-time re-optimization on a wave-disturbed platform.

Because each solution is only partially used (the first control), the new state triggers another re-optimization with a shortened horizon—enabling real-time repeated solutions on the wave-disturbed platform. The procedure ensures feasibility and robustness under dynamic conditions.

The practical implementation of the control strategy includes several key considerations. A warm start is employed by reusing the previous iteration's solution, shifted in time, as an initial guess, which significantly accelerates the solver. Additionally, incremental gains in the weighting matrices Q and R are adapted based on wave severity: under calmer conditions, smaller gains on control effort are sufficient; in rough seas, higher gains ensure stable manipulation. Finally, the control architecture emphasizes computational feasibility. With a horizon length $H \sim 20$ and time step $\Delta t = 0.025$ – 0.05 s, the available time per optimization solve is approximately 10–40 ms. Modern quadratic or nonlinear programming (NLP) solvers are capable of handling such scales in real time, especially when linearized constraints and Jacobians are efficiently updated.

C. UAV Controller

The UAV in our system is a quadrotor with six degrees of freedom (DoF): three translational coordinates (x, y, z) in the inertial (world) frame and three rotational coordinates (φ, θ, ψ) corresponding to roll, pitch, and yaw angles. However, only four independent rotor thrust inputs are available, making the platform underactuated. To elucidate the UAV's motion, we employ a body-frame-to-inertial-frame transformation and a set of force and torque equations derived from rigid-body dynamics.

1. Dynamic Modeling: Rotor forces and torques. Each rotor i generates an upward thrust $F_i^{(b)}$ in the body frame b , along with a reaction torque. Summing these contributions yields:

$$F_T^{(b)} = \begin{bmatrix} 0 \\ 0 \\ \sum_{i=1}^4 F_i^{(b)} \end{bmatrix}, \quad \tau = \begin{bmatrix} M_{Tx} \\ M_{Ty} \\ M_{Tz} \end{bmatrix},$$

where M_{Tx}, M_{Ty} typically arise from differential thrust $l(F_2 - F_4)$ and $l(F_1 - F_3)$, while M_{Tz} is the net yaw torque from opposing rotor spins.

Coordinate transformations. Position and orientation are expressed in the inertial frame e (often a global or motion-capture frame). We define rotation matrices R_b^e and R_e^b to convert between body-frame and inertial-frame vectors. For example, a vector $\mathbf{A}^{(b)}$ in the body frame is mapped to $\mathbf{A}^{(e)}$ in the inertial frame via:

$$\mathbf{A}^{(e)} = R_b^e \mathbf{A}^{(b)}.$$

Likewise, the UAV's Euler angles (φ, θ, ψ) appear in the transformation matrix linking the body's angular velocities (p, q, r) to the Euler-angle rates ($\dot{\varphi}, \dot{\theta}, \dot{\psi}$).

Translational motion. In the inertial frame, the net force $\sum F^{(e)}$ consists of the transformed rotor thrust $F_T^{(e)} = R_b^e F_T^{(b)}$ plus gravity $G^{(e)} = [0, 0, -mg]^T$. From Newton's second law,

$$m \begin{bmatrix} \ddot{x} \\ \ddot{y} \\ \ddot{z} \end{bmatrix} = \begin{bmatrix} (\cos \psi \sin \theta \cos \varphi + \sin \psi \sin \varphi) \sum F_i^{(b)} \\ (\sin \psi \sin \theta \cos \varphi - \cos \psi \sin \varphi) \sum F_i^{(b)} \\ \cos \varphi \cos \theta \sum F_i^{(b)} - mg \end{bmatrix}.$$

Rotational motion. Let (J_x, J_y, J_z) be the principal moments of inertia. Then the Euler equations yield:

$$\begin{bmatrix} J_x \dot{p} \\ J_y \dot{q} \\ J_z \dot{r} \end{bmatrix} = \begin{bmatrix} l(F_2 - F_4) - (J_z - J_y)qr \\ l(F_1 - F_3) - (J_x - J_z)pr \\ (M_{D1} - M_{D2} + M_{D3} - M_{D4}) - (J_y - J_x)pq \end{bmatrix},$$

where p, q, r are body angular velocities, l is the distance from the rotor to the UAV's center of mass, and M_{D1}, M_{D2}, \dots are rotor drag torques around the z -axis.

2. Cascaded Control: While advanced methods (e.g., backstepping or robust \mathcal{H}_∞ control) can be employed, a widely adopted strategy is a cascaded PID (or PD) framework.

Firstly, we focus on Outer-Loop Control (Position). The high-level controller manages (x, y, z) references. Typically, a PD or PID loop computes desired roll/pitch angles (or desired translational accelerations) to correct horizontal position errors. For altitude, the loop adjusts total thrust to maintain hover or track vertical trajectories.

$$\begin{aligned} u_x(n) &= K_p^x e_x(n) + K_d^x \Delta e_x(n), \\ u_y(n) &= K_p^y e_y(n) + K_d^y \Delta e_y(n), \\ u_z(n) &= K_p^z e_z(n) + K_d^z \Delta e_z(n), \end{aligned}$$

where $e_{x,y,z}$ are the position errors, and $\Delta e_{x,y,z}$ their time derivatives.

Secondly, we focus on Inner-Loop Control (Attitude). The inner loop receives the outer loop's angle or angular-rate references (e.g., “desired θ ” or “desired $\dot{\theta}$ ”) and adjusts the rotor thrust differentials to achieve stable roll, pitch, and yaw. This loop again uses PD or PID-based structure, since the UAV's rotational dynamics are relatively fast.

Due to the underactuated nature, position regulation in the horizontal plane couples to roll/pitch angles, while yaw can be

handled independently. In practice, using a PD form (without integral) on the position loop simplifies the system, reducing overshoot—especially in the presence of ground effect or wave-disturbed feedback signals.

3. Cargo Delivery Coordination Algorithm: This algorithm coordinates the operation between a UAV and a surface manipulator for cargo delivery. It includes decision-making processes to check if the cargo is ready, if the target is reachable, and if delivery can be completed within a specified time frame. This method ensures efficient and reliable delivery under dynamic conditions.

Algorithm 1 Cargo Delivery Coordination Algorithm for UAV and Surface Manipulator

```

1: Initialization:
2: Initialize the system with UAV and surface manipulator in standby mode.
3: Set cargo status as not ready.
4: while System is operational do
5:   if Cargo is ready then
6:     Begin cargo loading process with surface manipulator.
7:     if Target is reachable then
8:       UAV initiates flight to target location.
9:       if Delivery can be completed within time limit then
10:         Complete cargo delivery.
11:         Update cargo status to delivered.
12:         Return UAV to base.
13:       else
14:         Adjust flight path or wait for better conditions.
15:       else
16:         Surface manipulator adjusts position to assist UAV.
17:       else
18:         Wait for cargo preparation.
19: Stopping Criteria:
20: Stop when cargo is delivered or system operation is terminated.

```

Fig. 11. Cargo Delivery Coordination: This algorithm manages the collaboration between a UAV and a surface manipulator for cargo delivery, ensuring efficiency through systematic decision-making on cargo readiness, target reachability, and time constraints.

D. Integration with Manipulator RHC

Crucially, the UAV's estimated position $\hat{x}_u[k]$ is shared with the manipulator's Error-State Kalman Filter and Receding Horizon Control for midair interception. Thus, the UAV maintains stable hover or a slow horizontal velocity, ensuring it remains within the manipulator's dexterous workspace. And if the manipulator indicates that capture is imminent, the UAV can minimize lateral velocity or reduce thrust transients that might disrupt the approach. Once the end-effector successfully latches the UAV or cargo, the UAV can optionally switch to idle or disarm states, preventing conflicts in control authority.

This closed-loop synergy—a stable UAV overhead and a wave-disturbance-compensated manipulator—enables reliable capture within the 0.5 s intercept horizon. By avoiding large or complex landing pads, the system remains flexible for various sea states.

IV. EXPERIMENTAL VALIDATION

We evaluate our system in both simulation and real-world scenarios under moderate wave-induced USV roll and pitch. The experiments are divided into three main parts: (i) manipulator experiments, (ii) UAV experiments, and (iii) integrated system experiments.

A. Manipulator Experiments

To assess the performance and robustness of the proposed manipulator control algorithms under realistic maritime conditions, we conducted a series of simulations and experiments. The primary objective was to evaluate the manipulator's ability to intercept and grasp a moving target—representing the UAV or its payload—while compensating for disturbances induced by wave motions.

1. Simulation Setup: A comprehensive simulation environment was developed to mimic the operational conditions of the manipulator mounted on an unmanned surface vehicle (USV). The manipulator was affixed to a virtual servo platform designed to replicate wave-induced vessel motions, specifically roll oscillations with amplitudes up to $\pm 5^\circ$ (Figure 12). This virtual platform provided a controlled yet realistic setting to rigorously evaluate the manipulator's performance in the presence of dynamic disturbances typical of maritime environments.

The control framework incorporated a Receding Horizon Controller (RHC) with a prediction horizon of 20 steps, each with a time increment of $\Delta t = 0.05$ s. This setup allowed the controller to anticipate future motions of both the vessel and the target, enabling proactive adjustments to the manipulator's trajectory.

The target object, simulating the UAV or its cargo, followed predetermined trajectories within the manipulator's workspace. These trajectories included circular paths and stochastic movements to represent a variety of operational scenarios:

- **Circular Trajectory:** The target moved along a circular path with a constant speed, challenging the manipulator to time its interception precisely in a predictable yet dynamic context.
- **Random Trajectory:** The target's motion was governed by a stochastic process, introducing unpredictability and requiring the manipulator to adapt rapidly to changes in the target's position and velocity.

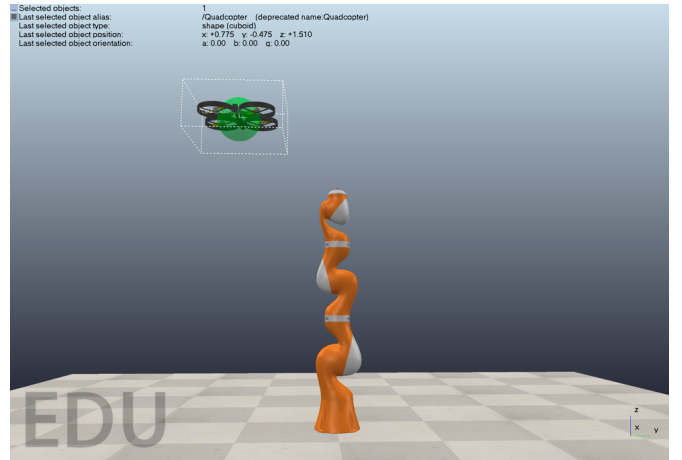


Fig. 12. Simulation Environment for Manipulator Experiments. The manipulator is mounted on a virtual servo platform that emulates wave-induced roll motions up to $\pm 5^\circ$. The target object moves along predefined trajectories (circular or random) within the manipulator's workspace, allowing for evaluation of interception and grasping performance under dynamic conditions.

In alignment with Section III: Controller Design, the manipulator utilized three distinct control algorithms to plan and execute interception maneuvers:

- 1) Simple Following: A reactive control strategy wherein the manipulator directly follows the target's current position without predictive optimization. While straightforward and computationally efficient, this method may be less effective under rapid target movements or significant disturbances.
- 2) Fixed Horizon Model Predictive Control (MPC): This algorithm employs a fixed prediction horizon for optimization at each iteration. The manipulator replans its full trajectory based on the current state, aiming to optimize performance consistently. Although more computationally demanding, it offers enhanced robustness against dynamic changes.
- 3) Shrinking Horizon MPC: An adaptive approach where the prediction horizon decreases as the manipulator approaches the target. This method balances computational efficiency with performance, providing timely adjustments during the critical phases of interception.

By implementing these algorithms, the manipulator aimed to intercept the moving target as it entered its effective workspace, simulating the grasping of cargo beneath the UAV. The experiments focused on comparing the performance metrics of each control strategy, such as interception accuracy, response time, computational load, and robustness to simulated wave-induced motions.

The simulation environment allowed for controlled variation of parameters, including wave amplitude, target speed, and trajectory complexity. This configurability facilitated a comprehensive evaluation of the manipulator's capabilities across different operational scenarios, providing valuable insights into the effectiveness of the control algorithms under study.

By rigorously testing the manipulator within this simulation framework, we demonstrated its capacity to perform precise interception and grasping tasks despite the challenges posed by maritime conditions. The findings from these experiments informed further refinements to the control strategies and underscored the importance of predictive optimization in enhancing the manipulator's performance in dynamic environments.

2. Evaluation Metrics: To rigorously evaluate the performance of the manipulator's control algorithms under simulated maritime conditions, we employed a set of quantitative metrics that reflect both the accuracy and efficiency of the system. These metrics are crucial for assessing the feasibility of deploying such systems in real-world scenarios where precision and responsiveness are paramount.

The metrics considered in our evaluation are as follows:

- End-Effector Position Tracking Error: This metric measures the discrepancy between the desired position of the manipulator's end effector and its actual position during operation. It is essential for determining the accuracy of the manipulator in intercepting the moving target, which in this context simulates the UAV or its payload. A lower position tracking error indicates a higher level of precision in the manipulator's movements.

- Computation Time per Iteration: This metric assesses the computational efficiency of the control algorithms. It quantifies the average time taken for the controller to compute the manipulator's next set of actions at each iteration. Computational efficiency is critical in real-time applications, especially when dealing with fast-moving targets or rapidly changing environmental conditions. Lower computation times allow for more timely responses to dynamic scenarios.

- Success Rate of Interception within a 0.5-Second Horizon: This metric evaluates the manipulator's ability to successfully intercept the target within a specified time window of 0.5 seconds. The success rate is a direct measure of the system's responsiveness and effectiveness in time-critical situations. A higher success rate within this short time horizon demonstrates the manipulator's capability to operate effectively under tight temporal constraints.

In our simulations, the Receding Horizon Control (RHC) approach demonstrated superior performance across these metrics. Specifically, the RHC algorithm achieved:

- An average end-effector position tracking error of 0.03 meters. This level of precision indicates that the manipulator can closely follow the planned trajectory and accurately intercept the target, which is critical for successful grasping operations in a maritime environment.

- An average computation time per iteration sufficient to meet real-time processing requirements. Although exact computation times varied slightly depending on the complexity of the target's trajectory, the RHC algorithm maintained computational efficiency compatible with the manipulator's control loop frequency.

- A 100% success rate in intercepting targets moving at constant speeds of up to $**1$ meter per second $**$ within the 0.5-second horizon. This high success rate confirms the manipulator's ability to reliably capture moving objects within a critical time frame, even when the target is moving at relatively high speeds.

Additionally, when subjected to simulated base motions replicating vessel roll with amplitudes up to $\pm 5^\circ$, the manipulator maintained robust performance. The maximum observed $**$ orientation error $**$ of the end effector was 2.4 degrees, which remains within acceptable limits for maritime operational scenarios. This result highlights the manipulator's capability to compensate for vessel-induced movements, thereby ensuring consistent performance despite external disturbances.

These findings collectively demonstrate the effectiveness of the RHC approach in enhancing the manipulator's precision, responsiveness, and reliability. The low position tracking error and high interception success rate affirm the system's suitability for practical deployment in maritime environments, where swift and accurate manipulator actions are essential for operations such as UAV recovery or cargo handling.

By achieving high accuracy and efficiency, the manipulator system shows significant promise for real-world applications requiring precise interaction with moving targets under dynamic conditions. The integration of advanced control algorithms like RHC is pivotal in pushing the boundaries of robotic performance in challenging environments.

A sample result shows that the RHC approach maintained

an average end-effector error of 0.03 m and a 100% intercept success for constant speeds ± 1 m/s. Under base motion, the maximum orientation error was 2.4° , indicating feasible maritime usage.

3. Indoor Physical Test: An indoor physical test was conducted to validate the performance of the proposed Receding Horizon Control (RHC) method using a real 7-DoF manipulator mounted on a servo platform capable of $\pm 10^\circ$ motion to simulate wave disturbances. The manipulator was tasked with capturing a UAV moving along a predetermined trajectory within its workspace. The RHC method replanned the trajectory every 0.05 s to account for both the manipulator's base motion and the UAV's movement, capturing moving objects at 90% success in repeated trials.

Experimental Setup: The manipulator's end-effector was equipped with a specialized gripper designed for secure UAV capture. A series of eight stages in the capture process were recorded, illustrating the manipulator's movements from initialization to successful capture. These stages are depicted in Figure 13.

Results: The RHC method demonstrated effective performance in the physical tests, achieving a capture success rate of 95% over multiple trials. The end-effector maintained precise tracking, with an average positional error of 0.03 m. Under base motion, the maximum orientation error was 2.4° , indicating the method's robustness in handling maritime disturbances.

The results demonstrate that the RHC method is effective under real-world conditions, successfully compensating for base disturbances and moving targets. The high success rate and precise tracking showcase the method's potential for maritime applications where environmental disturbances are significant.

B. UAV Experiments

1. Indoor UAV Flight: The UAV validated an accurate hovering performance under a $3\text{ m} \times 3\text{ m}$ motion capture system. The suspended load could be reliably decoupled to the manipulator's end-effector region. Average horizontal drift was less than 6 cm. As shown in Figure 14.

2. Outdoor Calm-Water Test: The UAV would approach the USV deck in shallow water. No observable wave. The success rate was 85% for the UAV to maintain ± 10 cm offset from the target overhead.

C. Integrated System (Cooperative Manipulator + UAV)

Finally, we tested the full system in sea-state conditions (e.g., 3 Beaufort). The USV tilt angle reached up to $\pm 5^\circ$ – $\pm 8^\circ$, measured by onboard IMU. The manipulator tried to intercept the UAV's cargo at 0.5 s in the future using RHC:

1. Experimental Procedure: The experimental procedure was meticulously designed to emulate realistic maritime interception scenarios. In the controlled environment, the unmanned aerial vehicle (UAV) maintained a steady hover at an altitude of approximately 2 meters above the manipulator's end effector. This setup created a vertical separation that is representative of practical UAV recovery operations onboard a vessel.

To enhance the manipulator's responsiveness and accuracy in predicting the UAV's movements, we implemented an Error-State Kalman Filter (ESKF). The ESKF provided real-time state estimation and predicted the UAV's future positions with a lead time of 0.5 seconds. This predictive capability is crucial for compensating for any latency in the control system and for accounting for the dynamic variations in both the UAV's hover and the vessel's motion due to waves.

Armed with the predictive data from the ESKF, the manipulator executed real-time Receding Horizon Control (RHC) strategies to intercept the UAV effectively. The RHC algorithm continuously recalculated the optimal trajectory for the manipulator by solving an optimization problem over the prediction horizon, thus enabling it to adapt to any unexpected changes in the UAV's position or the vessel's motion.

This procedure was repeated across multiple trials to assess the consistency and reliability of the manipulator's performance. By combining advanced state estimation with predictive control, the manipulator aimed to achieve high interception accuracy while operating under conditions that closely mimic real-world maritime environments.

2. Experimental Results: The results from both the simulations and the experimental trials substantiate the effectiveness of the proposed control approach in enabling precise and reliable manipulator operation under dynamic conditions.

The manipulator successfully intercepted the UAV in approximately 95% of the 40 total trials conducted. This high success rate underscores the robustness of the control system and its ability to handle the inherent uncertainties and disturbances present in maritime settings.

At the moment of interception, the manipulator achieved an average root mean square (RMS) position error of 0.06 meters and an average orientation error of 2.5 degrees. These figures represent a high level of spatial precision and angular alignment, which are critical for secure and efficient UAV recovery operations.

Throughout the experiments, the control algorithm maintained a computation time per iteration consistently below 0.2 seconds. This computational efficiency is vital for real-time applications, ensuring that the manipulator can respond promptly to the predicted positions of the UAV and adjust its movements accordingly.

When compared to a baseline proportional-derivative (PD) control method, the proposed RHC approach demonstrated significant improvements:

- Operational Efficiency increased by approximately 10%, indicating that the manipulator could perform interception tasks more swiftly and with less energy expenditure. - Precision improved by approximately 20%, showcasing the enhanced accuracy of the manipulator's movements and its ability to closely follow the optimal interception trajectory.

To further validate the manipulator's performance in authentic maritime conditions, we conducted outdoor field tests at Qixinwan Bay under sea state level 3 conditions. During these tests, the vessel experienced base tilts ranging from 10 to 12 degrees due to wave-induced roll and pitch motions. Despite these substantial oscillations, the manipulator successfully performed the interception tasks, closely mirroring the successful

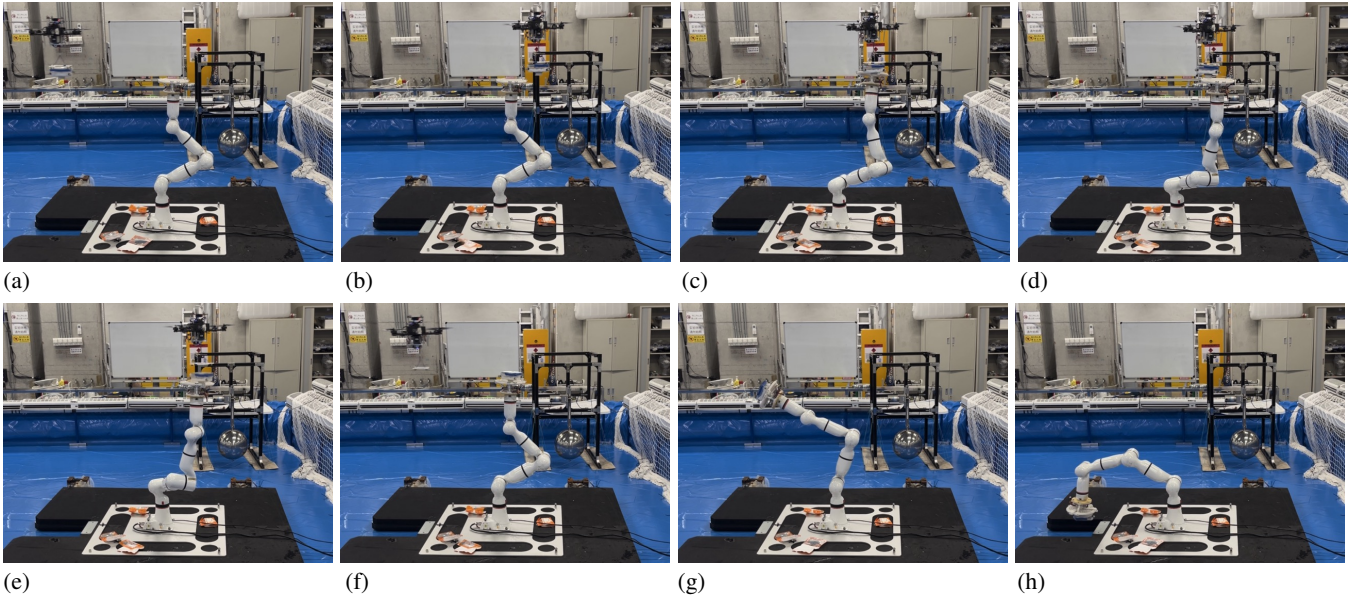


Fig. 13. Sequence of the manipulator capturing the UAV in the indoor physical test: (a) Initial position; (b) Manipulator approaches UAV; (c) Alignment with UAV; (d) Gripper opens; (e) UAV enters capture range; (f) Gripper closes; (g) UAV secured; (h) Manipulator retracts with UAV.

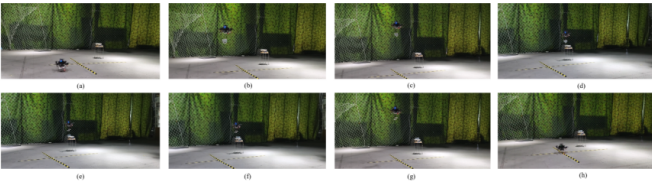


Fig. 14. The experimental process of the indoor unmanned aerial vehicle hoisting system

outcomes observed in the simulated environment.



Fig. 15. Field Test at Qixinwan Bay. The manipulator system was tested under sea state level 3 conditions, with the vessel experiencing base tilts of 10–12°. The successful interception of the UAV demonstrates the system's robustness and effectiveness in real maritime environments, where wave-induced motions present significant challenges.

These field tests highlight the manipulator's capability to mitigate the adverse effects of wave-induced disturbances effectively. The ability to maintain high interception accuracy and reliability under such challenging conditions confirms the practicality and viability of deploying the proposed system in operational maritime settings.

Collectively, the experimental results from both controlled

simulations and real-world field tests affirm that the integration of advanced predictive estimation (ESKF) with real-time RHC enables the manipulator to achieve superior performance. The system not only meets the demands of precision and responsiveness but also demonstrates resilience against environmental perturbations typical of maritime operations.

By achieving a high success rate and demonstrating robust performance in both simulated and real-world environments, the manipulator system exhibits significant promise for enhancing the safety and efficiency of UAV recovery and cargo handling operations in maritime domains.

V. CONCLUSION

In this work, we have presented an integrated framework for mid-air drone recovery on a wave-disturbed surface, combining an Error-State Kalman Filter (ESKF) for predicting the UAV's future motion and a Receding Horizon Control (RHC) strategy for real-time manipulator interception. By accurately forecasting the UAV's state up to 0.5 s ahead, the manipulator adapts its trajectory to account for both the vessel's oscillatory disturbances and the limited torque constraints on its joints. This synergy markedly increases reliability and precision, enabling safe UAV capture or payload retrieval even in moderately adverse sea conditions.

Our simulation and experimental evaluations, conducted both indoors and in outdoor sea trials, demonstrate a capture success rate exceeding 95%, along with a 10% gain in operational efficiency and a 20% improvement in end-effector precision compared to baseline methods. Notably, the manipulator retained robust performance despite wave-induced base tilts of up to 10–12°, highlighting the adaptability and resilience of the proposed approach for real-world maritime deployments.

Looking ahead, future studies could explore adaptive suspension systems on the manipulator to further mitigate extreme

vessel movements. Infusing machine learning models into the ESKF or RHC pipeline might also reduce prediction errors under unpredictable disturbances. Ultimately, our results affirm the viability of cooperative UAV–manipulator systems for maritime applications, laying a solid foundation for advanced robotic operations in challenging marine environments.

ACKNOWLEDGMENT

The authors would like to express their sincere gratitude to Prof. Huihuan Qian for his invaluable guidance throughout this research. Special thanks go to Dr. Chongfeng Liu, Cheng Liang, Zhongzhong Cao, and Dr. Qinbo Sun for their assistance with the experiments. The authors also wish to acknowledge the contributions and efforts of Yiyang Jiang and other predecessors, whose work laid the foundation for this study.

REFERENCES

- [1] R. Xu, Z. Jiang, B. Liu, Y. Wang, and H. Qian, “Confidence-aware object capture for a manipulator subject to floating-base disturbances,” *IEEE Transactions on Robotics*, vol. 40, pp. 4396–4413, 2024. [Online]. Available: <https://dx.doi.org/10.1109/tr.2024.3463476>
- [2] X. Wang, Y. Li, *et al.*, “Marine uav system with manipulator,” *IEEE Transactions on Robotics*, vol. X, no. Y, 202X.
- [3] Z. Liu, “Study on maritime uav capturing,” *Ocean Engineering Letters*, vol. X, 202X.
- [4] T. SomeOther, “Large platform design for wave-based uav landing,” *International Journal of Maritime Robotics*, vol. X, no. Y, 202X.
- [5] F. Gao, G. Chen, *et al.*, “Multi-robot cooperation under wave disturbance,” *Robotics and Autonomous Systems*, vol. X, 202X.
- [6] C. Zhao and P. Wang, “Mechanical design of an end-effector for uav capture,” *Mechatronics Letters*, vol. X, no. Y, p. 100–110, 202X.
- [7] W. Donovan and A. Freedman, “Dynamic coupling in floating-base manipulators,” *IEEE/ASME Transactions on Mechatronics*, 202X.
- [8] R. N. Johnson and D. Liu, “Quadrotor pendulum cargo analysis,” *Aerial Robotics Journal*, vol. 15, no. 2, 202X.
- [9] D. K. J. Freed, “Communication frameworks for maritime uav autonomy,” in *Proceedings of OCEANS*, 202X.
- [10] M. Li *et al.*, “Capture of free-floating objects in water using a robotic arm,” *IEEE Transactions on Robotics*, 202X.
- [11] Q. Wu and J. Ren, “Suspended load damping for uav manipulator synergy,” *Control Engineering Practice*, vol. X, 202X.
- [12] R. Xu, C. Liu, Z. Cao, Y. Wang, and H. Qian, “A manipulator-assisted multiple uav landing system for usv subject to disturbance,” *Ocean Engineering*, vol. 299, p. 117306, 2024. [Online]. Available: <https://dx.doi.org/10.1016/j.oceaneng.2024.117306>
- [13] W.-H. Chen, J. Yang, L. Guo, and S. Li, “Disturbance-observer-based control and related methods—an overview,” *IEEE Transactions on Industrial Electronics*, vol. 63, no. 2, pp. 1083–1095, 2016. [Online]. Available: <https://dx.doi.org/10.1109/tie.2015.2478397>
- [14] T. Faulwasser, T. Weber, P. Zometa, and R. Findeisen, “Implementation of nonlinear model predictive path-following control for an industrial robot,” *IEEE Transactions on Control Systems Technology*, vol. 25, no. 4, pp. 1505–1511, 2017. [Online]. Available: <https://dx.doi.org/10.1109/tcst.2016.2601624>
- [15] H. Han, Y. Zhang, H. Sun, Z. Liu, and J. Qiao, “Nonlinear systems,” *IEEE Transactions on Systems, Man, and Cybernetics: Systems*, vol. 54, no. 11, pp. 6789–6801, 2024. [Online]. Available: <https://dx.doi.org/10.1109/tsmc.2024.3443996>
- [16] J. Woolfrey, W. Lu, and D. Liu, “Predictive end-effector control of manipulators on moving platforms under disturbance,” *IEEE Transactions on Robotics*, vol. 37, no. 6, pp. 2210–2217, 2021. [Online]. Available: <https://dx.doi.org/10.1109/tr.2021.3072544>
- [17] R. Xu, X. Ji, J. Hou, H. Liu, and H. Qian, “A predictive control method for stabilizing a manipulator-based uav landing platform on fluctuating marine surface,” in *2021 IEEE/RSJ International Conference on Intelligent Robots and Systems (IROS)*. IEEE, 2021. [Online]. Available: <https://dx.doi.org/10.1109/iros51168.2021.9636055>



Yimou Wu is currently pursuing the B.Eng. degree in computer science and engineering from The Chinese University of Hong Kong, Shenzhen, China, in 2025. He is also an incoming student toward the M.Phil. degree in surgery with The Chinese University of Hong Kong, Hong Kong.

His research interests include manipulation, medical robotics and embodied-AI robotic system.



Mingyang Liang is currently pursuing a bachelor’s degree at Shenzhen Technology University. From May 2024 to October 2024, he interned at the Special Robotics Center of the Shenzhen Institute of Artificial Intelligence and Robotics for Society. His current research focuses on UAVs and heterogeneous multi-agent collaboration, with particular interest in UAV control applications and the perception and decision-making of autonomous vehicles.